Vol. 12, pp. 69–78 (2015)
doi: 10.2142/biophysico.12.0_69

Biophysics and Physicobiology
https://www.jstage.jst.go.jp/browse/biophysico/

Regular Article

Time-resolved chemiluminescence of firefly luciferin generated by dissolving oxygen in deoxygenated dimethyl sulfoxide containing potassium *tert*-butoxide

Yuki Yanagisawa[1], Kosuke Hasegawa[1], Naohisa Wada[2], Masatoshi Tanaka[1] and Takao Sekiya[1]

[1]*Department of Physics, Faculty of Engineering, Yokohama National University, Yokohama 240-8501, Japan*
[2]*Department of Food Life Sciences, Toyo University, Gunma 374-0193, Japan*

Received June 23, 2015; accepted October 16, 2015

Chemiluminescence (CL) of firefly luciferin (Ln) consisting of red and green emission peaks can be generated by dissolving oxygen (O_2) gas in deoxygenated dimethyl sulfoxide containing potassium *tert*-butoxide (*t*-BuOK) even without the enzyme luciferase. In this study, the characteristics of CL of Ln are examined by varying the concentrations of both Ln ([Ln]) and *t*-BuOK ([*t*-BuOK]). The time courses of the green and the red luminescence signals are also measured using a 32-channel photo sensor module. Interestingly, addition of 18-crown-6 ether (18-crown-6), a good clathrate for K^+, to the reaction solution before exposure to O_2 changes the luminescence from green to red when [*t*-BuOK] = 20 mM and [18-crown-6] = 80 mM. Based on our experimental results, we propose a two-pathway model where K^+ plays an important role in the regulation of Ln CL to explain the two-color luminescence observed from electronically excited oxyluciferin *via* dioxetanone.

Keywords: non-enzymatic color-tuning model, superoxide anion, dioxetanone, oxyluciferin, 18-crown-6 ether

Luminescence from firefly luciferin (Ln) can be classified into two types of reaction: (1) bioluminescence (BL), which occurs at the catalytic center of luciferase (Luc) in the presence of the cofactors Mg^{2+} and adenosine triphosphate (ATP), and (2) chemiluminescence (CL), which occurs in dimethyl sulfoxide (DMSO) in the presence of a strong base such as potassium *tert*-butoxide (*t*-BuOK). BL of Ln has a particularly high luminescence quantum yield of 41.0±7.4% [1], and the color of the luminescence can be tuned by altering conditions such as pH. Numerous researchers have attempted to explain the origin of this color-tuning mechanism. For example, White *et al.* [2,3] attributed this color tuning to the keto and enol tautomers of oxyluciferin in an excited state (Oxyln*) corresponding to the red and yellow-green emission signals, respectively. However, Branchini and coworkers [4] subsequently detected the yellow-green luminescence even from the keto form of 5,5-dimethyloxyluciferin (5,5-dimethylOxyln). McCapra *et al.* [5] performed quantum chemical calculations and proposed that the color of luminescence strongly depends on the conformation of Oxyln*. Their calculations suggested that Oxyln* with a planar structure could emit yellow-green light, whereas Oxyln* with a torsion angle of 90° around the single bond between the benzothiazole and thiazoline rings could emit red light. Nakatsu *et al.* [6] used the analog luciferyl-adenylate (Ln-AMP) to identify the catalytic center of Luc in *Luciola cruciata* (Genji Botaru in Japanese) including Oxyln through X-ray crystallography. They suggested that yellow-green light could be emitted if Oxyln* is firmly fixed by the chemical side chain of isoleucine, a hydrophobic amino acid residue in close proximity to the Luc catalytic center. Conversely, in the case of a mutant Luc, red light could be emitted if Oxyln* binds more loosely at its catalytic center because of the different hydrogen bond network between some amino acid residues from that of the wild type of Luc. Although various models have been proposed, a widely accepted model to explain the color tuning of firefly BL has not yet appeared. In the case of

Corresponding author: Naohisa Wada, Department of Food Life Sciences, Toyo University, 1-1-1 Izumino, Itakura-machi, Gunma 374-0193, Japan.
e-mail: bhwada@toyo.jp

CL, Seliger and McEloy [7] added Ln-AMP to DMSO at high pH to obtain bright CL.

Although our research group found that the BL of Ln initiated by ATP injection has a duration in the order of seconds [8], the generation mechanism of Oxyln* leading to BL has never been adequately elucidated because BL of Ln is a complex process. Therefore, in this study we clarify the elementary reaction process of Oxyln* without Luc; we focus on the much simpler CL system, where the CL reaction as a whole can be written as:

$$Ln + O_2 \xrightarrow{t\text{-BuOK}} Oxyln^* + CO_2. \quad (1)$$

Although reaction (1) is not catalyzed by Luc, both the red and the green luminescence peaks are detected. We use a vacuum system to evacuate oxygen (O_2) from DMSO in advance to prevent reactive oxygen species from initiating CL. This allows us to clarify the elemental processes of CL.

In DMSO containing *t*-BuOK, dissolved O_2 reacts with *t*-BuOK to produce the stable superoxide anion radical O_2^- [9,10], which is believed to be involved in the primary reaction process to generate Oxyln* [11]. Recently, Pinto da Silva and Esteves da Silva [12] performed calculations that indicated O_2^- could contribute to the CL reaction. Consequently, by simply evacuating O_2 from DMSO in advance, it is possible to measure the absorption and fluorescence spectra of the intermediates of Ln produced by mixing *t*-BuOK with DMSO containing Ln. We then pass dry O_2 gas through the solution containing the intermediates to measure the time-dependent changes of light intensity and spectra of Ln CL. Based on the resulting experimental data, we propose a model that could explain the color-tuning mechanism of CL caused by the interaction of ionized Oxyln* with the solvent molecules DMSO and *t*-BuOK.

Materials and Methods

The measurements were performed using a quartz cell designed to study the spectroscopic properties of Ln CL (Fig. 1). Experiments were performed at room temperature (20–25°C) inside a glove box filled with argon gas (humidity ≤30%). *t*-BuOK (Merck, USA) was placed in a small glass cylindrical cell and inserted into compartment A, and a solution of Ln (0.25 mM, Sigma, USA) in 0.2% hydrous DMSO (3.2 mL, Kanto Chemical, Japan) was placed in compartment B. In experiments using 18-crown-6 ether (Sigma), Ln in DMSO (1 mM, 0.8 mL) was placed in A and *t*-BuOK and 18-crown-6 in DMSO (2.4 mL) were placed in B. The concentrations of *t*-BuOK and 18-crown-6, hereafter denoted as n_B and n_C, respectively, used are listed in Table 1. The reaction cell was then connected to a vacuum system, which is shown in Figure 2. The solution was solidified using liquid nitrogen, and after evacuating to a pressure of 3×10^{-3} Pa to remove O_2 from DMSO, the solidified solution was melted and degassed. This freeze–pump–thaw cycle was repeated

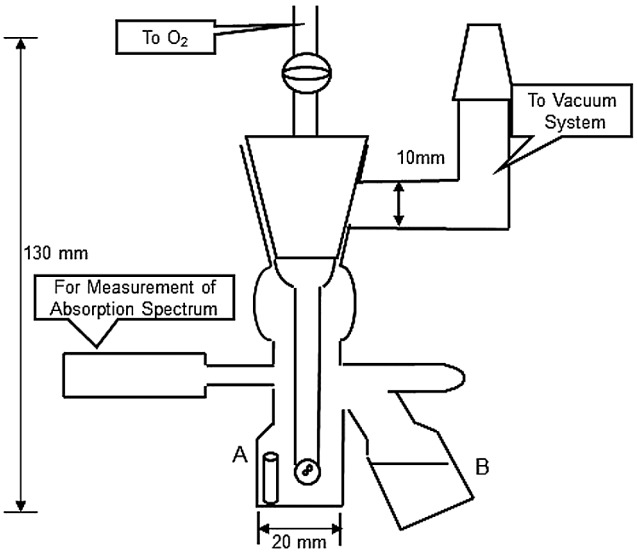

Figure 1 Reaction cell used for CL experiments.

three times in succession, after which the reaction cell was filled with argon at atmospheric pressure. Finally, the two solutions were mixed for ~30 min to give a homogenous solution.

O_2 gas was then dissolved into the mixed solution to measure the time course of the CL intensity, and the absorption and fluorescence spectra before and after initiating Ln CL. CL spectra were measured using a 32-channel photosensor module (H8353-02F, Hamamatsu Photonics, Hamamatsu, Japan) operated at 900 V at a sampling rate of 6,300 times every 100 ms. It should be noted that the small peak at ~660 nm detected in CL and fluorescence spectra is noise arising from a damaged channel in the 32-channnel module, so this peak should be ignored in the data (see Fig. 4 and 6–9). A flow of dry O_2 (200 mL/min) was introduced into the solution 20 s after starting detection. Absorption spectra were measured using a spectrometer (UV-365, Shimadzu, Kyoto, Japan) with a scan speed of 50 nm/min. A D_2/W lamp with a wavelength range of 280–600 nm was used as the light source. Fluorescence spectra were also measured using the 32-channel photosensor module operated at 500 V and a sampling rate of 100 times every 10 ms. The light source was a high-output violet light-emitting diode (λ=400 nm) (OSSV5111A, OptoSupply, Hong Kong). A glass filter (wavelength cut-off: λ<460 nm) was used in the fluorescence spectral measurements. The spectroscopic sensitivity of the

Table 1 Combinations of n_B and n_C applied in the CL experiments

n_B (mM)	n_C (mM)				
5	0				
10	0	10	20	40	
20	0	20	40	60	80
30	0	30	60	90	120

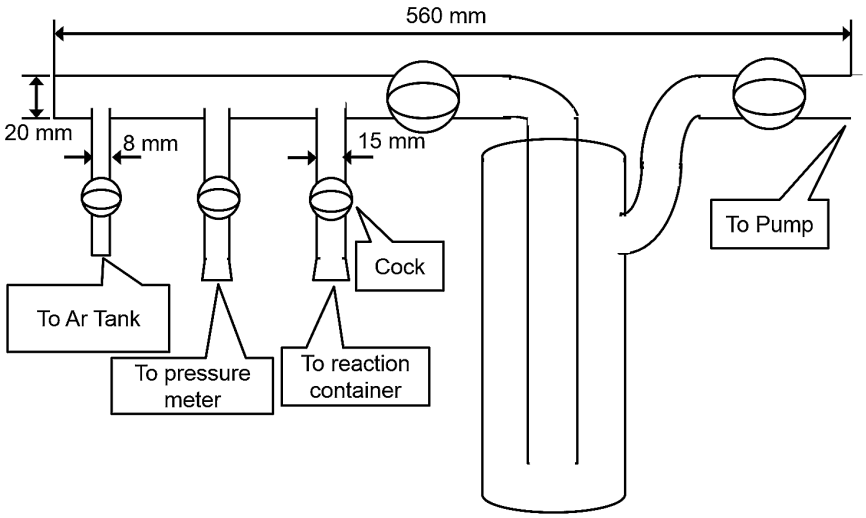

Figure 2 Vacuum system used to evacuate the reaction cell.

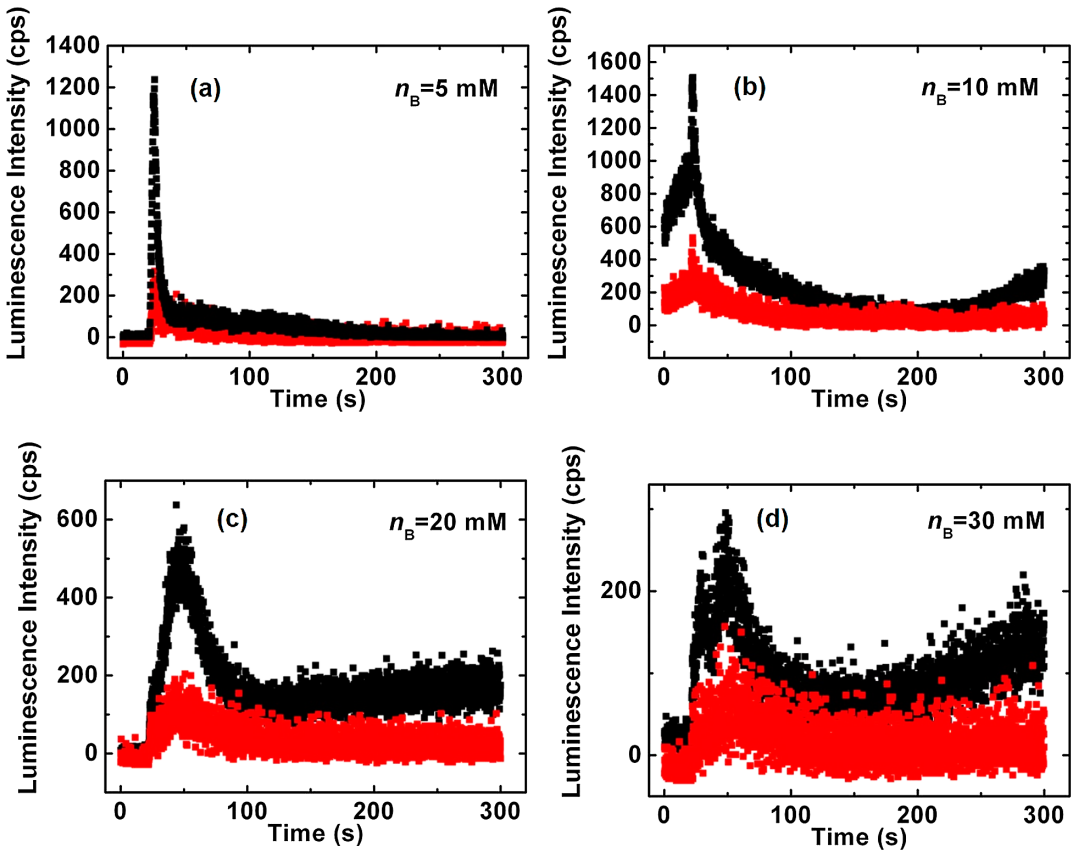

Figure 3 Dependence of the time courses of CL intensity on n_B of (a) = 5, (b) = 10, (c) = 20 and (d) = 30 mM. n_B is the concentration of *t*-BuOK. Black curve: λg ~520 nm. Red curve: λr ~620 nm. λg and λr are the peak wavelengths of the green and the red CL, respectively.

equipment was evaluated by comparison with the spectrum of the W lamp, and fluorescence and CL spectra were corrected. It should also be noted that the CL intensity was very weak compared with that of fluorescence. In our experimental conditions, this result can be explained reasonably as follows. The CL yield Φ_c is represented as:

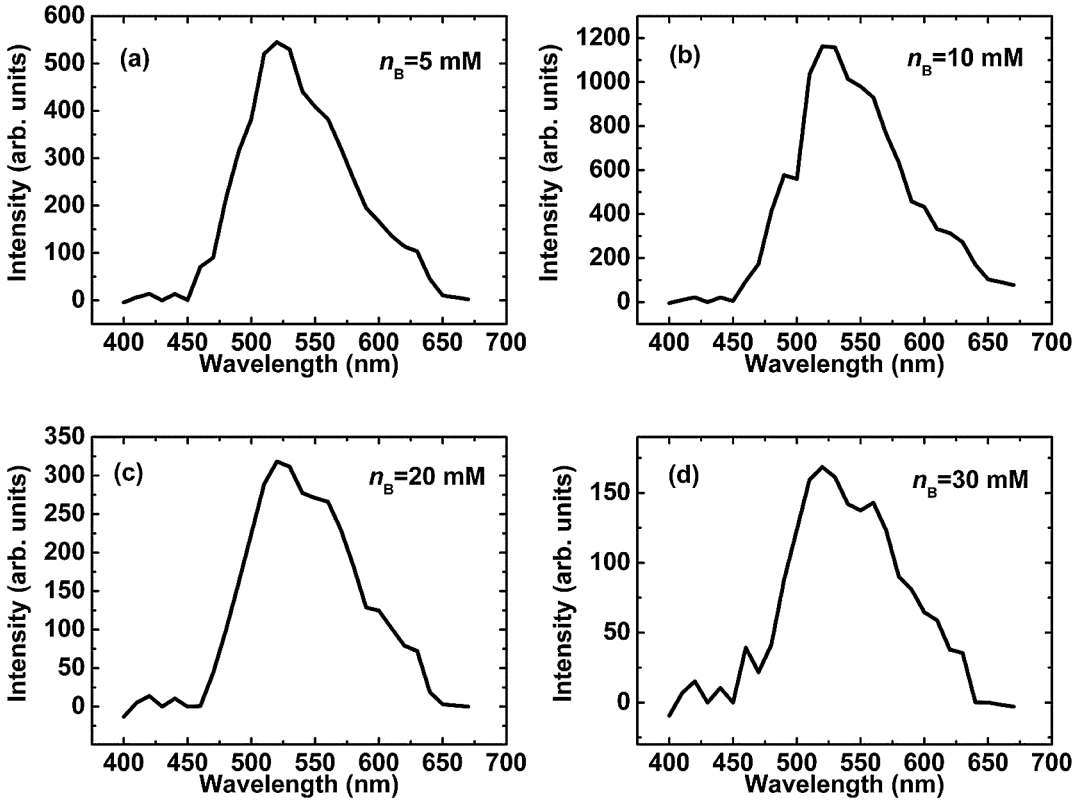

Figure 4 CL spectra obtained for n_B of (a) = 5, (b) = 10, (c) = 20 and (d) = 30 mM measured at the time when the luminescence peak appears. n_B is the concentration of *t*-BuOK.

$$\Phi_c = \Phi_{ne} \times \Phi_{na} \times \Phi_f, \quad (2)$$

where Φ_{ne} is non-enzymatic reaction yield, Φ_{na} is the probability of transition from the reactant in a ground state to the product in an electronically excited state, and Φ_f is fluorescence yield. Substituting the enzyme-specific reaction yield Φ_e for Φ_{ne} gives the BL yield Φ_b. In particular, it is known that Φ_c is much smaller than Φ_b when the luminescence and the fluorescence molecules are the same for BL/CL (*i.e.*, the same Φ_f), signifying $\Phi_{ne} << \Phi_e$.

Results and Discussion

Time course of CL intensity

When the time course of CL intensity was measured, green (λg~520 nm) and weaker red (λr~620 nm) emissions were observed regardless of n_B (Fig. 3). The strongest CL intensity was observed for n_B = 10 mM, and then its intensity weakened with increasing n_B. Figure 4(a)–(d) depict the CL spectra measured during the time of peak appearance (50–70 s) where the spectral shapes were the same for different n_B.

Next, we examined the effect of 18-crown-6 on the time course of CL intensity. For n_B = 10 mM, the time courses of the green and the red luminescence signals were not affected by changes of n_C, but the intensity of emission decreased with increasing n_C. For n_B = 20 mM, however, the time course of CL intensity (Fig. 5) and CL spectra measured during the time of peak appearance (50–70 s) (Fig. 6(a)–(c)), those of average intensity for the 50 s between 100–150 s (Fig. 6(d), (e)) and the time-dependent CL spectral changes for 70–150 s (Fig. 6(f)) exhibit different tendencies from each other. The peak intensity of the green luminescence at the time of the CL peak appearance was stronger than that of the red luminescence regardless of n_C. Comparing the time courses of CL intensity between n_C = 0 and 20 mM, the order of the intensity ratio of the green to the red luminescence remained unchanged until 300 s. Interestingly, a definite reversal of this intensity ratio was observed during 70–150 s when n_C = 80 mM (Fig. 5), corresponding to the CL spectral changes shown in Figure 6(f). This result indicates that 18-crown-6 could directly affect the CL spectra by scavenging K^+. Incidentally, the relative intensity of the green luminescence increases again in the period of 200–300 s for n_C = 80 mM; this is probably a secondary effect of 18-crown-6 but the mechanism of such behavior remains unclear.

It is currently unclear if the red luminescence originates from Oxyln itself. This is because singlet oxygen can emit very weak red light [13], so the contribution of singlet oxygen could not readily be excluded. Wada *et al.* [9,10] found that stable O_2^- is generated upon dissolving *t*-BuOK in de-

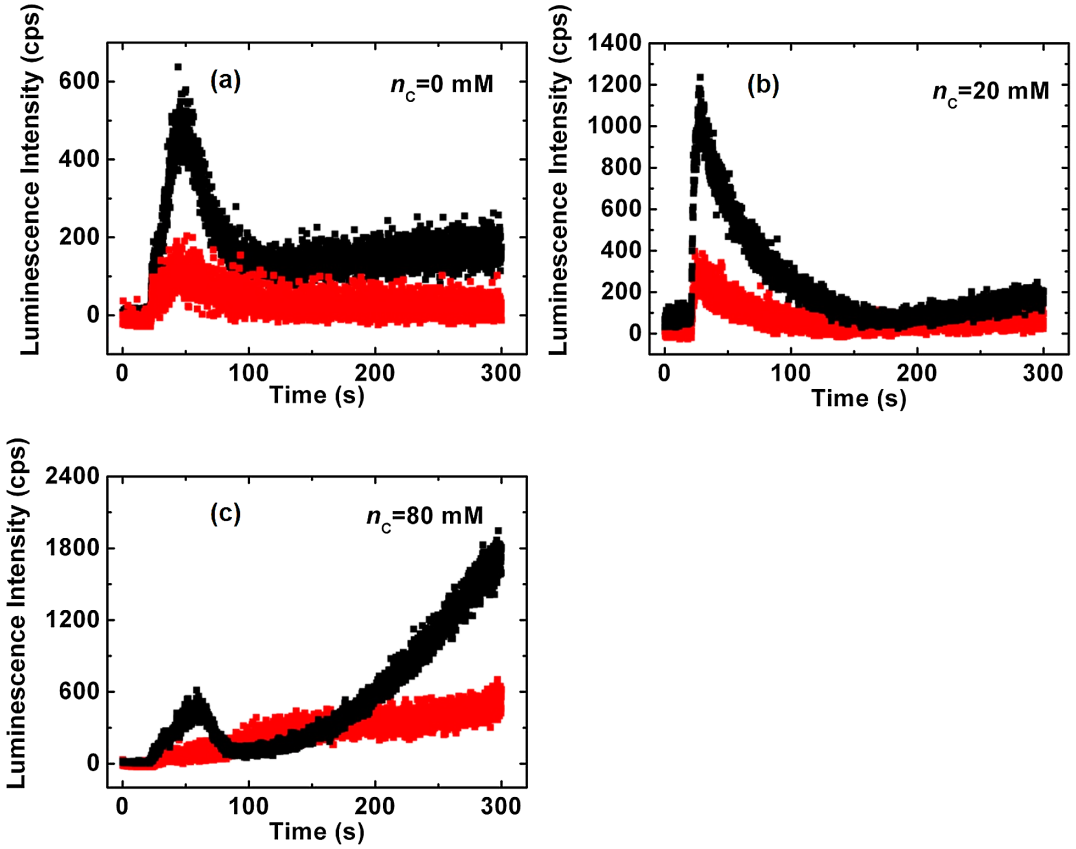

Figure 5 Time courses of CL intensity for n_B = 20 mM with increasing n_C of (a) = 0, (b) = 20 and (c) = 80 mM. n_B is the concentration of *t*-BuOK; n_C is the concentration of 18-crown-6. Black curve: λ*g* ~520 nm. Red curve: λ*r* ~620 nm.

oxygenated DMSO. O_2^- undergoes a bimolecular reaction to produce singlet oxygen in an excited state, emitting very weak red light. Therefore, it is important to confirm that the observed red luminescence is unique to Oxyln* and not produced by singlet oxygen. When *t*-BuOK alone (without Ln) was dissolved in deoxygenated DMSO, no red luminescence was observed when O_2 gas was passed through the solution. It was thus concluded that the red luminescence originates from Oxyln* in our system.

Absorption and fluorescence spectral changes before and after generating CL

Figures 7 and 8 show changes of absorption and fluorescence spectra before and after dissolving O_2 in reaction solutions with different combinations of n_B and n_C for 600 s. Regardless of n_B, the absorption peaks before generating CL were located at ~420 nm (Fig. 7(a)). After generating CL from the solutions with n_B = 5 and 10 mM, which exhibited more intense red luminescence than green luminescence, the absorption peaks shifted markedly to ~520 nm. Meanwhile, for the solutions with n_B = 20 and 30 mM, where there was no reversal in the relative intensities between the green and the red luminescence signals, the absorption peaks shifted to slightly shorter wavelength (Fig. 7(b)).

In the fluorescence spectra, peaks before generating CL appeared at ~560 nm (Fig. 7(c)). After generating CL from the solutions with n_B = 5 and 10 mM, the fluorescence intensity ratios of green-to-red emission reversed and the peak shifted markedly to ~620 nm. For the solutions with n_B = 20 and 30 mM, where there was no change in the relative intensity of the green and red CL, the fluorescence peak still remained at ~560 nm (Fig. 7(d)).

Next, we studied the effect of 18-crown-6 on the absorption and fluorescence spectra before and after dissolving O_2 in the reaction solutions. In the case of n_B = 10 mM, the absorption peak remained at ~420 nm (~520 nm) before (after) exposure to O_2. Even when n_C was increased, the same tendency was observed as when n_C = 0 mM (Fig. 7(a), (b)). Similarly, the fluorescence spectra appeared at ~560 nm (~620 nm) before (after) exposure to O_2 regardless of n_C (Fig. 7(c), (d)). Namely, 18-crown-6 did not affect the absorption and fluorescence spectra for the solution with n_B = 10 mM.

The absorption and fluorescence spectra for solutions with n_B = 20 mM and n_C = 40, 60 and 80 mM were also measured, but remarkable spectral changes were detected only for the 80 mM case. For the solution with n_C = 80 mM, before O_2 exposure, the absorption peak at ~420 nm shifted to a slightly

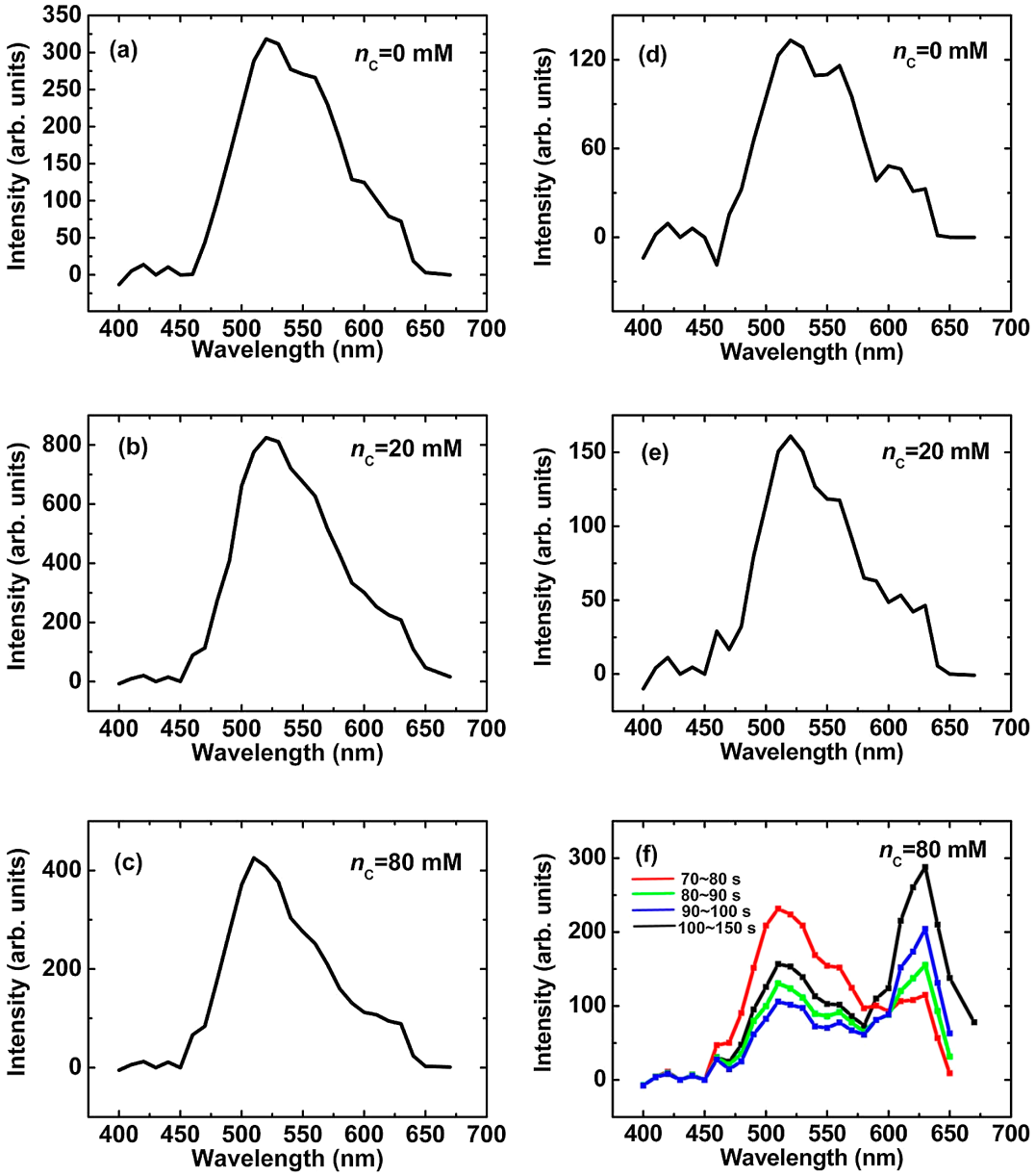

Figure 6 Time-dependent CL spectra with n_B = 20 mM for n_C of (a), (d) = 0, (b), (e) = 20 and (c), (f) = 80 mM. Data in (a)–(c) were measured at the time when the luminescence peak appears during the period of 50–70 s, and the average intensity of the peaks for the 50 s between 100–150 s are shown for n_C of (d) = 0 and (e) = 20 mM. (f) Time-dependent CL spectra with n_B=20 mM and n_C = 80 mM, where spectral changes are depicted in 10-s increments from 70 to 100 s along with the averaged CL spectrum over 100–150 s. n_B is the concentration of *t*-BuOK; n_C is the concentration of 18-crown-6.

shorter wavelength (Fig. 8(a)). After exposure to O_2, the intensity of the absorption peak at ~520 nm increased markedly (Fig. 8(b)). It is thus concluded that K^+ may play an important role as a regulation factor in the CL reaction pathway.

Concerning the fluorescence spectra before O_2 exposure, all the peaks at ~560 nm could be assigned to Ln independent of n_C (Fig. 8(c)). After exposure to O_2, the fluorescence peak for the solution with n_C = 20 mM remained at ~560 nm, whereas a large red shift to ~620 nm was observed for the solution with n_C = 80 mM (Fig. 8(d)), which was correlated with the corresponding absorption peak shift.

Regarding the solutions with n_B = 30 mM, before exposure to O_2, absorption peaks appeared at ~350 and ~420 nm and shifted to shorter wavelength with increasing n_C. After exposure to O_2, the intensity of the absorption peak at ~350 nm decreased, and the shift of the peak at ~420 nm was similar to the case before O_2 exposure. In contrast, the fluorescence peaks at ~560 nm were not affected by n_C and exposure to O_2.

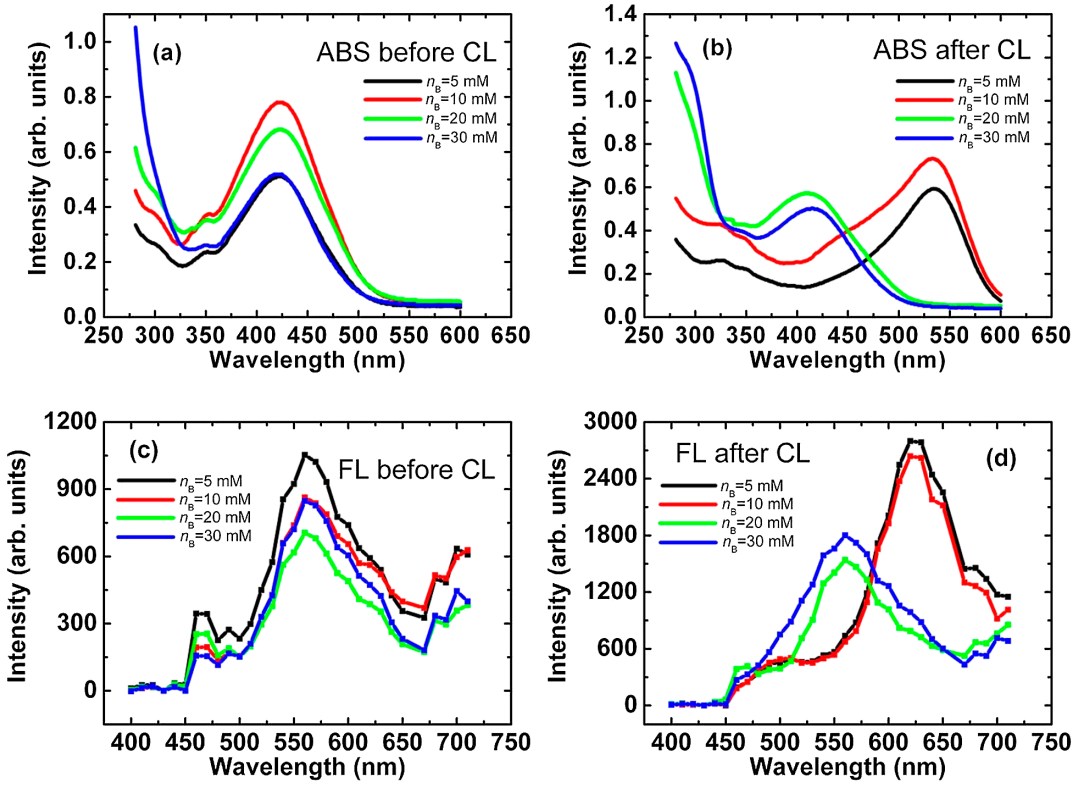

Figure 7 Dependence of (a), (b) absorption (ABS) and (c), (d) fluorescence (FL) spectral changes on n_B before and after exposure to O_2 without 18-crown-6. n_B is the concentration of *t*-BuOK.

Absorption and fluorescence spectral changes during O_2 exposure

Figure 9 displays the time dependence of the absorption and fluorescence spectra during O_2 exposure for a solution with n_B = 10 mM without 18-crown-6. The absorption peaks at ~420 nm before exposure to O_2 were assigned to Ln. On dissolving O_2 in the reaction solution, the peak at ~420 nm initially shifted to a slightly shorter wavelength, but then it moved to a longer wavelength and its intensity decreased. Moreover, a new peak appeared at ~520 nm from 140 s that continuously increased in intensity. At 270 s, the ratio of the relative intensities of the absorption peaks at 420 and 520 nm reversed with an isosbestic point at ~475 nm. The fluorescence peak at ~560 nm assigned to Ln remained until 90 s after exposure to O_2, and new peaks then appeared at ~520 and ~620 nm that grew monotonically. The ratio of the relative intensities of the fluorescence peaks at 520 and 620 nm reversed at 220 s. Thus, we can describe the Ln spectral changes leading to CL as follows. i) Regarding the spectral changes before and after exposure to O_2, the absorption and fluorescence peaks before O_2 exposure appeared at ~420 and ~560 nm, respectively, regardless of n_B. Because these peaks appeared before initiating CL, they can be regarded not as products of the CL reaction but as a remnant of Ln. However, for solutions with n_B = 20 and 30 mM before O_2 exposure, addition of 18-crown-6 caused the absorption peaks to shift to slightly shorter wavelength, and this shift could be induced by 18-crown-6 (Fig. 8(a)). ii) In the case of solutions with n_B = 5 or 10 mM without 18-crown-6, the absorption and fluorescence peaks were observed at ~520 and ~620 nm, respectively, after exposure to O_2. These peaks could be identified as Oxyln species that emit red light. iii) As shown in Figure 9, the time-dependent spectral changes upon exposure to O_2 imply that Oxyln species emitting green light could contribute to the absorption peak at ~420 nm and fluorescence peak at ~520 nm.

A two-pathway model for Ln CL

Our experimental results indicated that increasing n_B decreases the CL intensity; the peak intensity of CL was highest for n_B = 10 mM, and both the green and the red luminescence signals were observed simultaneously (Fig. 3). Because the low-intensity red luminescence became too weak to detect as n_B increased, it was likely that K^+ directly affected the primary process of the CL reaction. Therefore, we checked whether K^+ could be trapped by 18-crown-6 to affect the CL reaction. In the presence of 18-crown-6, the red luminescence was observed stably when n_B = 20 mM and n_C = 80 mM (Fig. 6(f)). We also confirmed that singlet oxygen was not the origin of the red luminescence in our system. We thus concluded that CL is composed of two emission colors and increasing the concentration of K^+ suppresses the inten-

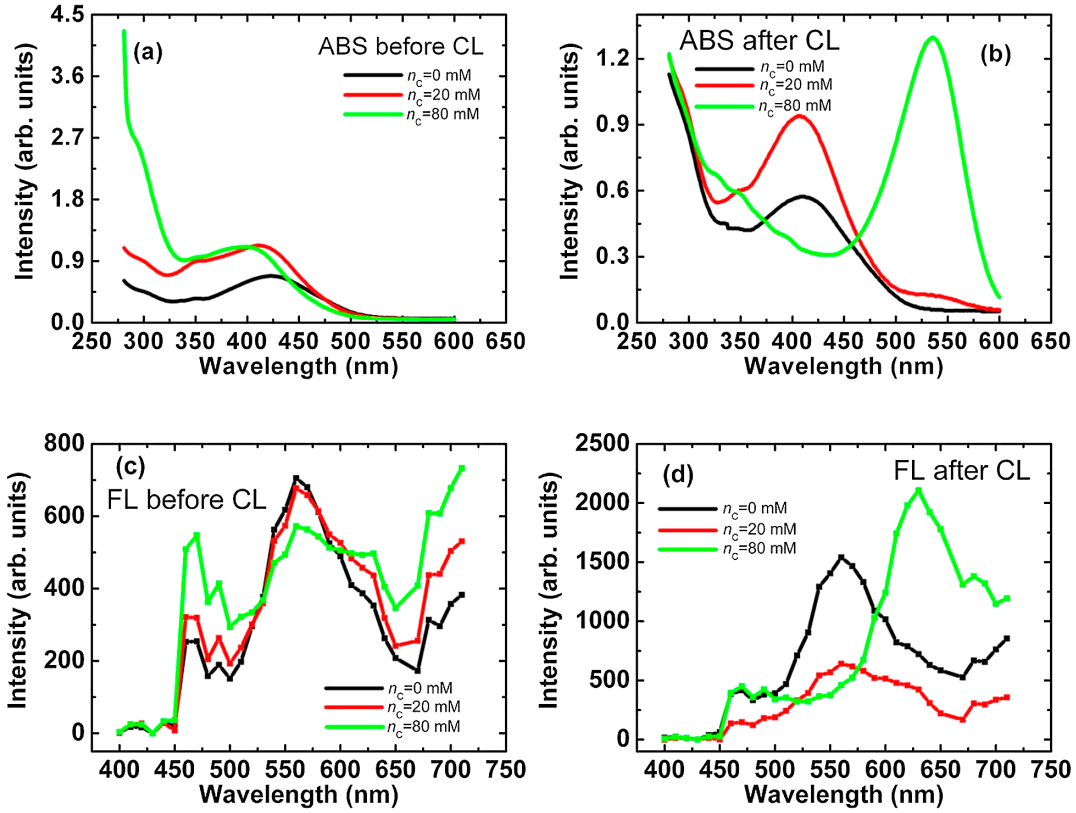

Figure 8 Dependence of (a), (b) absorption (ABS) and (c), (d) fluorescence (FL) spectral changes on n_C before and after exposure to O_2 for n_B = 20 mM. n_B is the concentration of *t*-BuOK; n_C is the concentration of 18-crown-6.

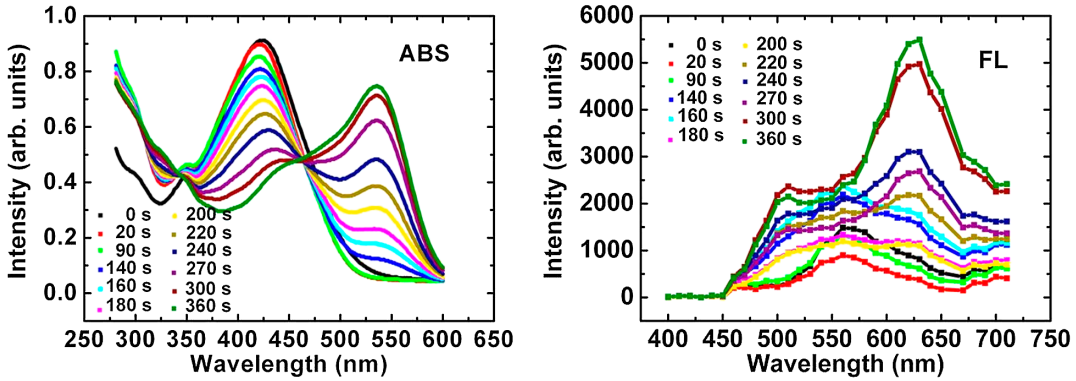

Figure 9 Changes in the absorption (ABS) (left) and fluorescence (FL) (right) spectra depending on the O_2 exposure time for n_B = 10 mM without 18-crown-6. n_B is the concentration of *t*-BuOK.

sity of the red luminescence.

Concerning the emitter in the BL reaction, Naumov *et al.* [14,15] proposed that the Oxyln species emitting red light is in the phenolate–keto form and that emitting yellow-green light is in the phenolate–enol or enolate form. Our main supposition is that in the case of BL, which is different from Ln CL, factors such as amino acid residues in proximity to the Luc catalytic center and the specific interactions with AMP and oxygen must be also considered [16,17]; this heterogeneous reaction field surrounding Oxyln* in Luc might affect the relaxation process of Oxyln* in a different way from that in CL. In fact, the BL peak appears at λ~560 nm [8] using a two-liquid mixing method where two sample solutions are injected quickly into the reaction vessel, but the CL peak measured in this study was λ*g*~520 nm, which is at considerably shorter wavelength than the BL peak. We propose a

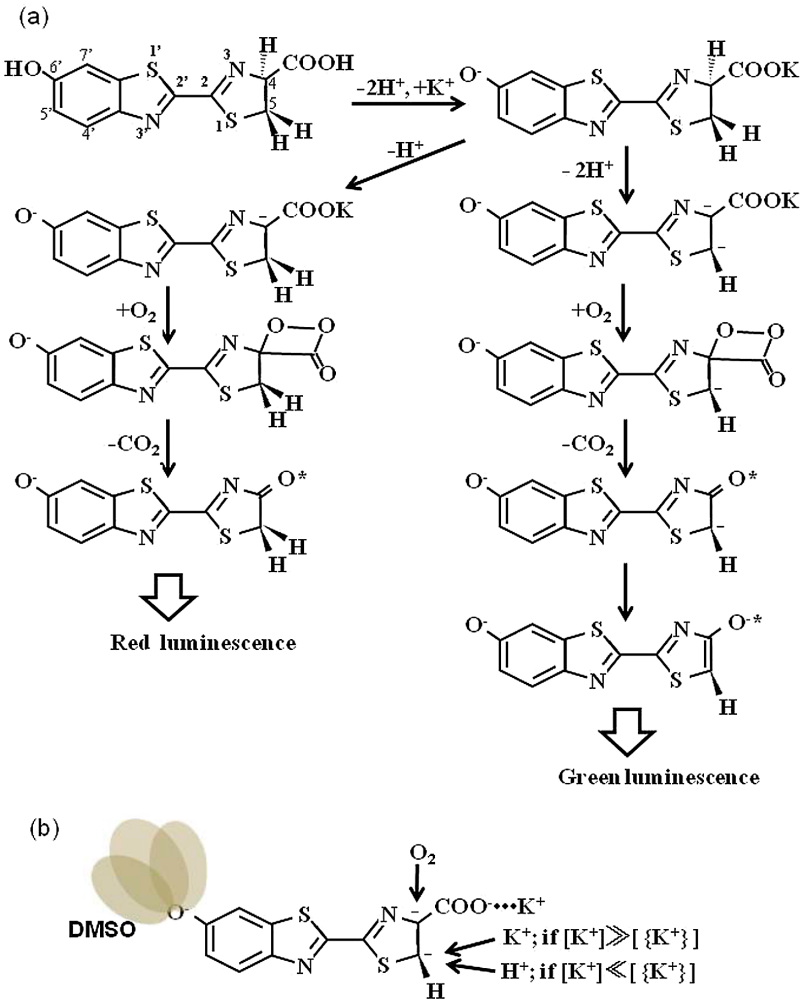

Figure 10 (a) Two-pathway model for firefly luciferin CL, and (b) the characteristics of microenvironmental interactions between Oxyln, O_2, K^+ and DMSO. Precursors of the green- and the red-light emitters are assumed to be generated prior to the formation of dioxetanone. Concentrations of free and 18-crown-6-bound K^+ are defined as $[K^+]$ and $[\{K^+\}]$, respectively.

two-pathway model that can lead to both the green and the red luminescence signals to reasonably explain our experimental findings (Fig. 10). Figure 10(a) and (b) show the elementary reaction pathways for our model leading to species that emit green and red light, and microenvironmental interactions between Oxyln, O_2, K^+ and DMSO, respectively.

First, considering the green emitter in the pathway in Figure 10(a), McCapra *et al.* [18] supposed the acidity of the C_5 site in Ln to be so large that Oxyln in the phenolate–enolate form could be generated if deprotonation occurs at the C_5 site by a certain basic amino acid residue in the catalytic center of Luc. Accordingly, if we apply this mechanism of formation of Oxyln that emits the green luminescence to our model, the emitter could be assigned to Oxyln* in the phenolate–enolate form. Second, concerning 5,5-dimethylOxyln, Hirano *et al*. [19] comprehensively measured absorption and fluorescence spectra using several types of organic bases in various solvents, from which they proposed the existence of a contact ion pair (CIP) or ion pair with a solvent molecule interposed between 5,5-dimethylOxyln and its counter ion (SSIP). In particular, it was assumed that both CIP and SSIP forms of 5,5-dimethylOxyln exist in DMSO because the polarity (dielectric constant) of this solvent has a mean value between that of a nonpolar solvent and polar solvent. Accordingly, in our two-pathway model, we hypothesized a state of ionization for each functional group, as shown in Figure 10(b). 1) The phenolic hydroxyl group is considered to be deprotonated at O^-, but a SSIP is formed by the steric effect of bulky DMSO; 2) –COOH is also deprotonated, but similar to the formation of the adenylate compound assisted by the divalent ion Mg^{2+} in the enzymatic reaction, a CIP could then be formed through electrostatic interaction involving K^+; 3) Deprotonation also occurs at C_4 synergistically with 2), and K^+ access must be prevented by the bulky DMSO such that it is easy for the neutral oxygen molecule to attack C_4; 4)

Whether or not one of the C_5 protons dissociates is considered to depend on the density of K^+ in its proximity. The relative quantity of free K^+ might decrease if there is excess 18-crown-6, so H^+ dissociation at C_5 site hardly occurs, leading to the red luminescence.

Based on the above considerations, the elementary reaction pathway splits before the production of the key molecule dioxetanone, and the proportion of the red to the green emissive Oxyln* species is regulated directly by K^+. Consequently, an excess of K^+ promotes deprotonation at the C_5 site of Ln, resulting in the green luminescence. Conversely, a low concentration of K^+ stabilizes protonation at the C_5 site, so the reaction pathway to the red luminescence could be unlocked. The observed effect of 18-crown-6 on the CL spectra can be explained reasonably by this model. Specifically, the experimental results obtained for $n_B = 20$ mM and $n_C = 80$ mM indicated that trapping of K^+ by 18-crown-6 could lower the effective concentration of free K^+. As a result, the reaction channel resulting in the red luminescence could be detectably facilitated.

In conclusion, we proposed a two-pathway model that could reasonably explain the experimental results for Ln CL. The main difference between CL and BL in the elementary reaction processes in our model is that when there is an excess of K^+ (*i.e.*, n_B is high), one of the protons at the C_5 site of Ln could dissociate in the primary step of the CL reaction.

Acknowledgments

The authors thank Mr. Shibata for his great contribution to the early stage of this work.

Conflict of Interest

All the authors declare that they have no conflict of interest.

Author Contributions

N. W. directed the project. M. T. and T. S. contributed to the experiments including design and construction of the experimental setups. Y. Y. and K. H. performed experiments and data analysis. Y. Y., N. W. and M. T. proposed a two-pathway model for Ln CL.

References

[1] Ando, Y., Niwa, K., Yamada, N., Enomoto, T., Irie, T., Kubota, H., *et al.* Firefly bioluminescence quantum yield and colour change by pH-sensitive greer emission. *Nat. Photonics* **2**, 44–47 (2008).

[2] White, E. H., Rapaport, E., Hopkins, T. A. & Seliger, H. H. Chemi- and bioluminescence of firefly luciferin. *J. Am. Chem. Soc.* **91**, 2178–2180 (1969).

[3] White, E. H., Steinmetz, M. G., Miano, J. D., Wildes, P. D. & Morland, R. Chemi- and bioluminescence of firefly luciferin. *J. Am. Chem. Soc.* **102**, 3199–3208 (1980).

[4] Branchini, B, R., Murtiashaw, M. H., Magyar, R. A., Portier, N. C., Ruggiero, M. C. & Stroh, J. G. Yellow-green and red firefly bioluminescence from 5,5-dimethoxyluciferin. *J. Am. Chem. Soc.* **124**, 2112–2113 (2002).

[5] McCapra, F. Mechanisms in chemiluminescence and bioluminescence unfinished business. In: *Bioluminescence and Chemiluminescence*, Hastings, J. W., Kricka, L. J. & Stanley, P. E., eds., Jhon Wiley & Sons, Chichester, U.K. pp. 7–15 (1996).

[6] Nakatsu, T., Ichiyama, S., Hiratake, J., Saldanha, A., Kobashi, N., Sakata, K., *et al.* Strauctural basis for the spectral difference in luciferase bioluminescence. *Nature* **440**, 372–376 (2006).

[7] Seliger, H. H. & McElroy, W. D. Chemiluminescence of firefly luciferin without Enzyme. *Science* **138**, 683–685 (1962).

[8] Yanagisawa, Y., Kageyama, T., Wada, N., Tanaka, M. & Ohno, S. Time courses and time-resolved spectra of firefly bioluminescence initiated by two methods of ATP injection and photolysis of caged ATP. *Photochem. Photobiol.* **89**, 1490–1496 (2013).

[9] Wada, N., Mitsuta, K., Kohno, M. & Suzuki, N. ESR studies of firefly D-(-)-luciferin chemiluminescence in dimethyl sulfoxide. *J. Phys. Soc. Jpn.* **58**, 3501–3504 (1989).

[10] Wada, N. & Mitsuta, K. Generation mechanism of the superoxide ion in the dimethyl sulfoxide solution dissolving potassium *t*-butoxide. *J. Phys. Soc. Jpn.* **62**, 1816–1817 (1993).

[11] Wada, N., Shibata, R., Shibazaki, M. & Suzuki, N. X-ray photoelectron valence band studies on firefly D-(-)-luciferin. *Photochem. Photobiol.* **49**, 513–518 (1989).

[12] Pinto da Silva, L. & Esteves da Silva, J. C. G. Theoretical study of the correlation between superoxide anion consumption and firefly luciferin chemiluminescence. *Chem. Phys. Lett.* **577**, 127–130 (2013).

[13] Khan, A. U. & Kasha, M. Physical theory of chemiluminescence in systems evolving molecular oxygen. *J. Am. Chem. Soc.* **88**, 1574–1576 (1965).

[14] Naumov, P., Ozawa, Y., Ohkubo, K. & Fukuzumi, S. Structure and spectroscopy of oxyluciferin, the light emitter of the firefly bioluminescence. *J. Am. Chem. Soc.* **131**, 11590–11605 (2009).

[15] Naumov, P. & Kochunnoonny, M. Spectral-structural effects on the keto-enol-enolate and phenol-phenolate equilibria of oxyluciferin. *J. Am. Chem. Soc.* **132**, 11566–11579 (2010).

[16] Milne, B. F., Marques, M. A. L. & Nogueira, F. Fragment molecular orbital investigation of the role of AMP protonation in firefly luciferase pH-sensitivity. *Phys. Chem. Chem. Phys.* **12**, 14285–14293 (2010).

[17] Sakai, H. & Wada, N. Full-quantum chemical calculations of the absorption maxima of oxyluciferin in the catalytic center of firefly luciferase containing adenosine monophosphate. *Comput. Theor. Chem.* **1045**, 93–98 (2014)

[18] McCapra, F. M. & Perring, K. D. Luciferin bioluminescence. In *Chemi- and Bioluminescence*. (Burr, J. G. ed.) pp. 359–383 (Marcel Dekker, Inc., New York, 1985)

[19] Hirano, T., Hasumi, Y., Ohtsuka, K., Maki, S., Niwa, H., Yamaji, M., *et al.* Spectroscopic studies of the light-color modulation mechanism of firefly (beetle) bioluminescence. *J. Am. Chem. Soc.* **131**, 2385–2396 (2009).